Effective interaction energy of water dimer at room temperature: An experimental and theoretical study

T. Nakayama,[a] H. Fukuda, T. Kamikawa, Y. Sakamoto, A. Sugita, and M. Kawasaki[b]
Laboratory of Photochemical Reaction, Department of Molecular Engineering, Kyoto University, Kyoto 615-8510, Japan

T. Amano, H. Sato, and S. Sakaki
Laboratory of Molecular Theory for Science and Technology, Department of Molecular Engineering, Kyoto University, Kyoto 615-8510, Japan

I. Morino
National Institute for Environmental Studies, Tsukuba 305-8506, Japan

G. Inoue
Graduate School for Environmental Studies, Nagoya University, Nagoya 464-8601, Japan

(Received 29 May 2007; accepted 26 July 2007; published online 2 October 2007)

Buffer-gas pressure broadening for the $\nu_1+\nu_3$ band of H_2O at 1.34–1.44 μm for a variety of buffer gases was investigated at room temperature using continuous-wave cavity ring-down spectroscopy. The effective interaction energy of water dimer under room temperature conditions was evaluated from the pressure broadening coefficients for rare gases using Permenter-Seaver's relation. Monte Carlo simulations were performed using *ab initio* molecular orbital calculations to evaluate the interaction energies for the water dimer at 300 K. In this theoretical calculation, the orientations of the two water molecules were statistically treated. © *2007 American Institute of Physics*.
[DOI: 10.1063/1.2773726]

I. INTRODUCTION

Water dimer, $(H_2O)_2$, has an important role in the radiation budget of the terrestrial atmosphere because of continuum absorptions in the visible, ultraviolet, and thermal infrared region.[1,2] Hence, it is essential to evaluate an accurate value for the abundance at atmospherically relevant temperatures. Experimental studies on the interaction energy of H_2O have been performed with two methods, thermal conductivity[3] and infrared absorption.[4–8] The dimerization enthalpies determined from thermal conductivity and infrared spectra are for the optimum structure. Theoretical studies have also been reported.[9–11] Usually, theoretical reports are based on the standard *ab initio* molecular orbital (MO) calculations and only one optimized configuration with the minimum energy is considered, which corresponds to the "frozen" structure at 0 K. A combination of Monte Carlo (MC) simulations and *ab initio* MO calculation enabled us to evaluate the temperature dependence of the interaction energies. Bandyopadhyay *et al.*[9] performed multicanonical MC simulations of the water dimer over a wide range of temperatures with the interaction computed by *ab initio* MO methods, but the level of their computation, RHF, might not be accurate enough to evaluate the small interaction energy of the water dimer.

In the present work, the effective interaction energy of the water dimer at room temperature was evaluated with pressure broadening measurements using Permenter-Seaver's relation.[12,13] We have measured the pressure broadening coefficients in the $\nu_1+\nu_3$ band of H_2O at 1.34–1.44 μm with noble gases as well as N_2 and O_2 with cavity ring-down spectroscopy (CRDS) using a tunable diode laser. First, the present experimental results were compared with the HITRAN database and the available literature data to check the reliability of our CRDS system. Second, the effective interaction energy at room temperature for $(H_2O)_2$ has been obtained by applying an energy transfer model to the observed pressure broadening coefficients of H_2O for noble gases. Finally, we have evaluated the interaction energies by using the MC simulation based on the *ab initio* MO calculation.

II. EXPERIMENTAL AND THEORETICAL METHODS

The experimental setup used in the present study is similar to that descried in our previous studies.[14] An external cavity diode laser (Santec Co., TSL-210V) was used as the near-infrared light source. The output laser beam, deflected by an acousto-optical modulator (Isomet), was directed into an optical cavity that consisted of two high reflectivity mirrors (II-VI Optics or Kuramoto Co.) with a separation of 60 cm. One of the two mirrors was incorporated in a tube-type piezoactuator (Piezomechanik, HPSt 150/20) for cavity length modulation, with a rate of about 300 Hz. The transmitted light from the cavity was directed to an InGaAs photodiode detector (Hamamatsu Photonics, G5851-11) attached to a preamplifier (NF, SA220F5). When the transmitted beam reached a threshold level, the deflected beam was switched

[a]Present address: Solar-Terrestrial Environment Laboratory and Graduate School of Science, Nagoya University, Furocho, Chikusa-ku, Nagoya 464-8601, Japan.
[b]Author to whom correspondence should be addressed. Fax: +81-75-383-2573; Electronic mail: kawasaki@moleng.kyoto-u.ac.jp

off by the acousto-optical modulator crystal and the light stored within the cavity started to ring down.

In the presence of an absorbing species, the light intensity within the cavity is given by the expression

$$I(t) = I_0 \exp(-t/\tau) = I_0 \exp(-t/\tau_0 - \sigma N c t), \quad (1)$$

where I_0 and $I(t)$ are the light intensities at time 0 and t, τ is the cavity ring-down time in the presence of an absorbing sample, τ_0 is the cavity ring-down time without the absorber present (typically 1.2 μs), and c is the velocity of light. N and σ are the concentration and absorption cross section of the absorbing species, respectively. The exponential decay data were digitized with an analog to digital converter (National Instruments, NI5122 100 MHz, 14 bits) and processed using LabVIEW software. Our program averaged the profile of several ring-down wave forms, for which individual ring-down decay curves except for the very initial part of the decay were fitted to a single-exponential function. Sixteen ring-down events were averaged for each spectral data point, thus, a complete scan took about 5–10 min.

Pressure broadening by various buffer gases (N_2, O_2, He, Ne, Ar, Kr, and Xe; 60–500 Torr) was measured at a fixed partial pressure of H_2O (0.04 Torr). Three or four measurements of the spectra were performed at each pressure condition. The gases (except Kr and Xe) were flowed with the use of mass-flow controllers (Kofloc, model 3660). Pressure and temperature of the sample gases in the cavity were monitored by pressure gauges (MKS, Baratron 622) and thermocouples, respectively, at the monitor ports. All experiments were performed at 298±2 K.

We performed the MC simulation combined with the *ab initio* MO method to evaluate the interaction energies of water dimer. The metropolis algorithm with the standard umbrella sampling technique was used to generate various configurations of water dimer at 300 K. The geometry of the molecule is fixed at the experimental one (R_{OH}=0.9579, ∠HOH=104.5°). MP2/6-31++G(d,p) level of computation was employed to evaluate the interaction energy at each configuration. The effective interaction energy was then computed as the statistical average over these configurations. Mrazek and Burda[15] suggested that this level of *ab initio* MO computations provided reasonable accuracy for the interaction energy. We would like to emphasize that this is a reliable computational level from the standpoint that thousands of configurations are needed to be sampled to evaluate the averaged interaction. Although it is time consuming compared to empirical force field or to Hartree-Fock method, the electron correlation often plays a crucial role to evaluate the accurate interaction energy.

III. RESULTS AND DISCUSSION

A. Pressure broadening coefficients for N_2, O_2, air, and noble gases: A comparison with the HITRAN database

The database for the pressure broadening coefficients in the near-infrared region has been accumulated with the use of Fourier transform spectroscopy (FTS) and tunable diode laser spectroscopy (TDLS). To check the reliability of our CRDS measurements, the air-broadening coefficients were compared with the HITRAN database[16] and available literature data.[17,18] An example of the measured profile for the $(J'_{K'_aK'_c}\text{-}J''_{K''_aK''_c})=(10_{37}\text{-}9_{36})$ transition of the $\nu_1+\nu_3$ band of H_2O, which was broadened by 210 Torr of Kr, is shown in the inset of Fig. 1, in which the best-fit Voigt profile is shown by the solid curve. The Gaussian component was constrained to the room temperature Doppler width. The data obtained for the half-width at half maximum (HWHM) of the Lorentzian component are plotted as a function of buffer gas pressure. A straight-line fit provides the pressure broadening coefficient γ in units of cm^{-1} atm^{-1}, as shown in Fig. 1. A small contribution (<2%) of self-broadening was taken into account.

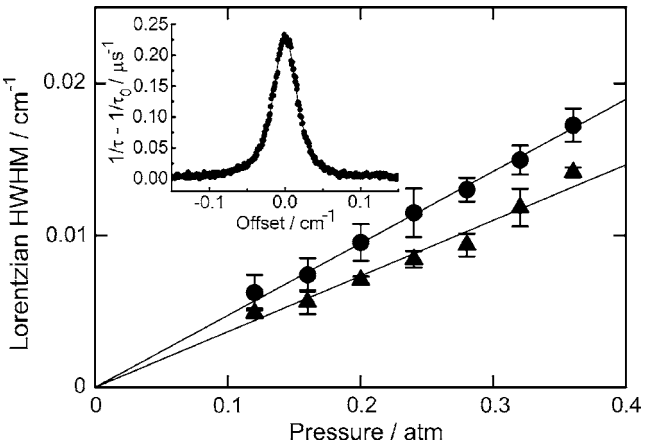

FIG. 1. Lorentzian widths (HWHM) for the $(10_{37}\leftarrow 9_{36})$ transition of the $\nu_1+\nu_3$ band of H_2O at 298 K as a function of pressure of buffer gases. Error bars indicate one standard deviation determined by the profile-fit procedure. ●: Kr, ▲: Ar. The inset shows an absorption profile for the $(10_{37}\leftarrow 9_{36})$ transition of the $\nu_1+\nu_3$ band of H_2O broadened for 210 Torr of Kr at 298 K. Filled circles represent experimental data. The solid curve represents a calculated spectrum with the Voigt function.

The obtained γ values of H_2O for various buffer gases, N_2, O_2, He, Ne, Ar, Kr, and Xe, are listed in Table I. We calculated the air-broadening coefficients γ(air) using the relation $\gamma(\text{air})=0.79\gamma(N_2)+0.21\gamma(O_2)$, which are listed in Table I and plotted as a function of the rotational quantum number index (m) and quasiquantum number (K_a) in the upper and lower panels in Fig. 2, respectively. The following index, m, was used to treat simultaneously the P- and R-branch transitions:

$$2m = J'(J'+1) - J''(J''+1),$$

$$P\ \text{branch}(J''-1 \leftarrow J''), \quad m = -J'',$$

$$R\ \text{branch}(J''+1 \leftarrow J''), \quad m = J''+1.$$

The data for the transitions of $K'_a=K''_a=2$, $\Delta K_a=0$ and $m=9$, $\Delta K_a=0$ were plotted in the upper and lower panels in Fig. 2, respectively. The HITRAN database[16] (solid line) and available literature data reported by Toth[17] based on FTS (triangles) and Liu *et al.*[18] based on TDLS (inverted triangles) are also plotted. Our values are in good agreement with the HITRAN database,[16] and the literature data reported by Toth[17] and Liu *et al.*[18]

TABLE I. Buffer-gas pressure broadening coefficients γ, in the unit of cm^{-1} atm^{-1} for H_2O at 298 K. (Numbers in parentheses are one standard deviation obtained by the straight-line fitting in units of the last digits quoted.)

Transition[a] $J'_{k'_a k'_c}$-$J''_{k''_a k''_c}$	N_2	O_2	Air[b]
5_{23}-6_{24}	0.0968(50)	0.0729(60)	0.0918(43)
5_{32}-4_{13}	0.1034(44)	0.0594(23)	0.0942(35)
9_{27}-8_{26}	0.0774(34)	0.0411(23)	0.0698(27)
10_{19}-9_{18}	0.0450(27)	0.0236(27)	0.0405(22)
10_{28}-9_{27}	0.0784(37)	0.0391(17)	0.0702(29)
10_{37}-9_{36}	0.0988(30)	0.0503(28)	0.0886(25)
10_{46}-9_{45}	0.0854(29)	0.0390(34)	0.0757(24)
10_{55}-9_{54}	0.0750(24)	0.301(23)	0.0656(20)
11_{29}-10_{28}	0.0662(30)	0.0293(16)	0.0585(24)
12_{210}-11_{29}	0.0606(43)	0.0217(29)	0.0524(34)

Transition $J'_{k'_a k'_c}$-$J''_{k''_a k''_c}$	He	Ne	Ar	Kr	Xe
5_{23}-4_{04}	0.0217(17)	0.0230(13)	0.0420(18)	0.0522(21)	0.0618(25)
10_{37}-9_{36}	0.0283(12)	0.0219(27)	0.0356(13)	0.0465(32)	0.0694(30)
10_{55}-9_{54}	0.0135(31)	0.0142(11)	0.0242(22)	0.0358(27)	0.0522(20)

[a]The rotational quantum numbers are in standard asymmetric rotor notation.
[b]Calculated from $\gamma(\text{air})=0.79\gamma(N_2)+0.21\gamma(O_2)$.

B. Experimental determination of the effective interaction energy of water dimer at 298 K

The effective interaction energy of $(H_2O)_2$ was evaluated using the observed broadening coefficients for noble gases. Broadening coefficients for noble gases for the $(5_{23}\leftarrow 4_{04})$, $(10_{37}\leftarrow 9_{36})$, and $(10_{55}\leftarrow 9_{54})$ transitions of the $\nu_1+\nu_3$ band were used for the evaluation. Permenter and Seaver[19,20] have developed a successful model that correlates Boltzmann averaged cross sections σ_M of a variety of energy transfer processes for a variety of collision partners M, with the intermolecular well depths ε_{AM}, for the interaction between the molecule A and a collision partner M.

$$\sigma_M = C\exp(\varepsilon_{AM}/k_BT), \tag{2}$$

where C is a constant, k_B is Boltzmann's constant, and T is temperature. The correlation is particularly useful for energy transfer processes which depend upon long range attractive forces. In the Lorentz-Berthelot geometric mean approximation, $\varepsilon_{AM}=(\varepsilon_{AA}\varepsilon_{MM})^{1/2}$, the equation is conveniently expressed in terms of the well depth ε_{AA} for the dimer of A and ε_{MM} for the dimer of M,

$$\ln(\sigma_M) = \ln C + (\varepsilon_{AA}/k_BT^2)^{1/2}\times(\varepsilon_{MM}/k_B)^{1/2}. \tag{3}$$

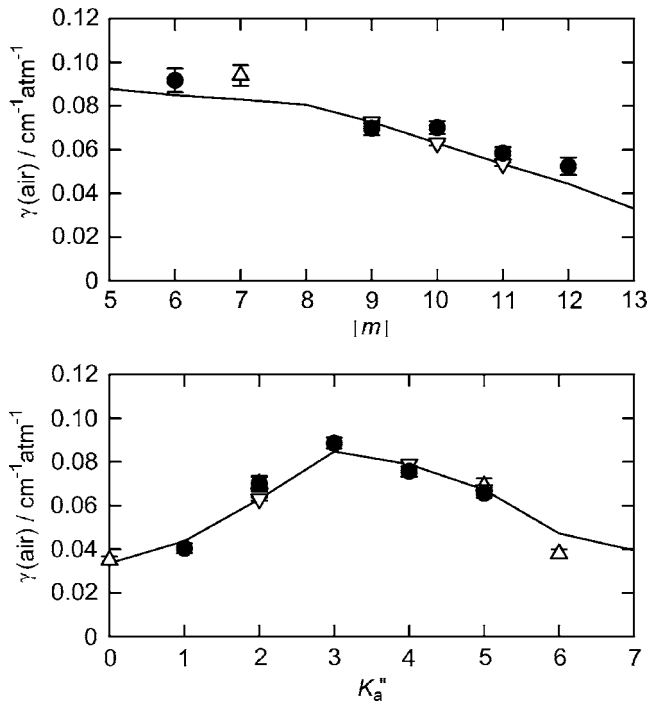

FIG. 2. Pressure broadening coefficients of H_2O for air as a function of (upper panel) rotational level $|m|$ for $K'_a=K''_a=2$, and (lower panel) quasi-quantum number K''_a for $\Delta K_a=0$ with $m=9$. ●: This work, ▽: Toth (Ref. 17), △: Liu *et al.* (Ref. 18), solid line: HITRAN (Ref. 16). Error bars indicate one standard deviation determined by the profile-fit procedure.

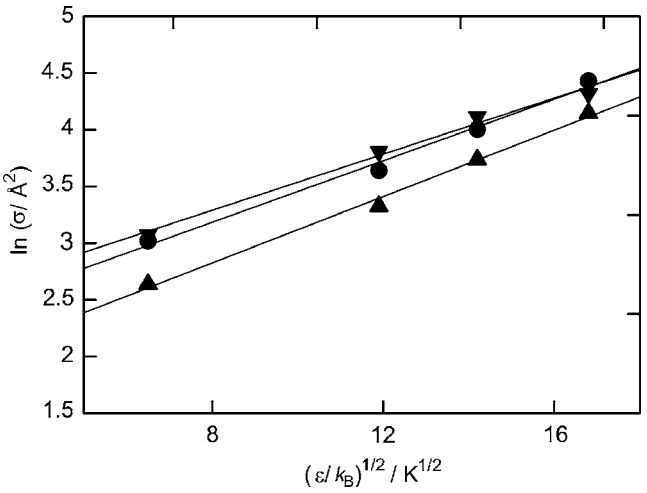

FIG. 3. Plots of the logarithm of the cross section σ_M for the broadening process of the $(5_{23}\leftarrow 4_{04})$ (inverted triangles), $(10_{37}\leftarrow 9_{36})$ (circles), and $(10_{55}\leftarrow 9_{54})$ (triangles) transitions of the $\nu_1+\nu_3$ band vs the well depth ε_{MM} of the dimer of a variety of noble gases (filled circles: Ne, Ar, Kr, and Xe). Solid lines show the results of a linear least-squares fit of the experimental data. See Eq. (3).

Figure 3 shows the Permenter-Seaver plots for the pressure broadening of the $(5_{23}\leftarrow 4_{04})$, $(10_{37}\leftarrow 9_{36})$, and $(10_{55}\leftarrow 9_{54})$ transitions of the $\nu_1+\nu_3$ band for a variety of colliding rare gases ($\varepsilon_{NeNe}/k_B=42.31$ K, $\varepsilon_{ArAr}/k_B=143.33$ K, $\varepsilon_{KrKr}/k_B=201.43$ K, and $\varepsilon_{XeXe}/k_B=282.88$ K). These ε_{MM}/k_B data are taken from the best estimated values compiled by Tang and Toennies.[21] In Fig. 3, σ_M is the cross section for the broadening process calculated by converting γ to SI units and multiplying by the factor $2\pi k_BT/\langle v_r\rangle$. As shown in Fig. 3, a linear correlation is observed for Ne, Ar, Kr, and Xe. Linear least-squares fit analysis of the data in Fig. 3 yielded the effective intermolecular well depth (interaction energy at room temperature) for $(H_2O)_2$ to be $\varepsilon_{H_2OH_2O}/k_B=1360\pm200$, 1630 ± 180, and 1900 ± 210 K for $(5_{23}\leftarrow 4_{04})$, $(10_{37}\leftarrow 9_{36})$, and $(10_{55}\leftarrow 9_{54})$ transitions, respectively. We chose to cite a final value, the average of the individual determinations together with error limits, which encompass the extremes of the determinations, hence, $\varepsilon_{H_2OH_2O}/k_B=1630\pm480$ K (3.24 ± 0.95 kcal mol^{-1}).

TABLE II. Dimerization enthalpies and effective interaction energies of H_2O dimer.

Method	$\varepsilon_{H_2O\text{-}H_2O}$ (kcal mol^{-1})	Reference
(Experimental)		
Thermal conductivity	3.59±0.50[a]	3
Infrared absorption	5.20±1.50[a]	4
Infrared absorption	4.55[a]	5
Infrared absorption	3.98±0.90[a]	6
Infrared absorption	3.6±0.7[a]	7
Infrared absorption	3.80±0.07[a]	8
Pressure broadening	3.24±0.95[b]	This work
(Theoretical)		
MC simulation[c]	3.32[d]	This work

[a]Previous reported values of dimerization enthalpy.
[b]Effective interaction energy for 298±2 K.
[c]Monte Carlo simulation combined with the *ab initio* molecular orbital method. An evaluated zero point energy of 1.22 kcal mol^{-1} was taken into account (see text).
[d]Effective interaction energy for 300 K.

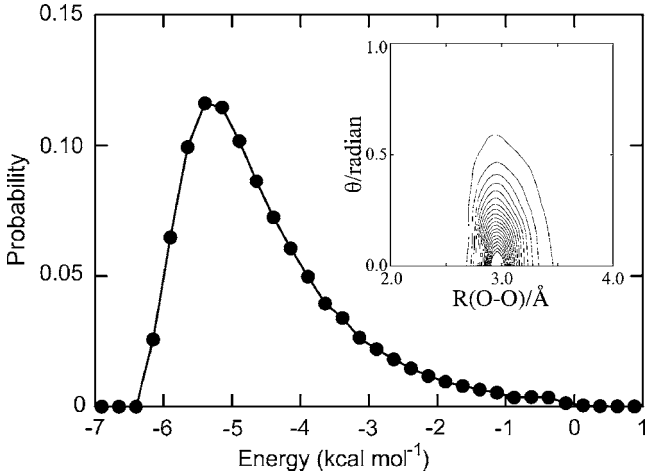

FIG. 4. The distribution of the interaction energies at 300 K determined by Monte Carlo simulation using *ab initio* molecular orbital calculation for various configurations of the two H_2O molecules. The insert shows the distribution function of dimer configurations for the O–O distances and the angles of the H(hydrogen bonding)–O–O.

The obtained experimental result was listed in Table II with the selected literature experimental data of the dimerization enthalpy of H_2O. The present results provide the effective interaction energy of H_2O dimer at room temperature. Our experimental value, 3.24±0.95 kcal mol^{-1}, is smaller by 0.35–1.96 kcal mol^{-1} than the recent experimental data. This difference could be attributed to the fact that the reported dimerization enthalpy was obtained for the minimum energy geometry in the thermal conductivity and infrared absorption measurements, while our experimental result was obtained for an average over the different orientations of the two colliding water molecules at 298 K, an atmospheric relevant temperature.

C. Theoretical calculations of the effective interaction energy of water dimer at 300 K

The integration over various configurations using molecular simulation technique such as MC is necessary to compare with the experimental estimation. Figure 4 shows the distribution of the interaction energy at 300 K. The distribution is typical in the canonical distribution and shows qualitative agreement with that by Bandyopadhyay *et al.*,[9] although they did not show the absolute value. Note that the levels of *ab initio* computations are different between their simulation and ours, and their energy using RHF/6-31G* slightly underestimates the binding energy. It is noteworthy that the depth shows significant temperature dependence,[22] that is, the distribution of the interaction energy is shifted to positively greater (shallower) direction with increasing temperature due to the thermal energy in the vibrational modes. The averaged interaction energy from our simulation is −4.54 kcal mol^{-1}, in which the zero point energy (ZPE) is neglected. The ZPE of the geometry-optimized dimer is 1.22 kcal mol^{-1}. Since ZPEs cannot be evaluated at arbitrary configurations except for the minimum, we estimate the effective interaction energy with the ZPE correction by simply adding the aforementioned ZPE. Our best theoretical estimation of the effective interaction energy at 300 K is, thus, 3.32 kcal mol^{-1}. This value agrees well with the experimental one within the margin of the experimental error. It should be noted, however, that a few sources of errors still remain that are difficult to be estimated. One is the basis set superposition error (BSSE) and the other is the contribution from the geometrical relaxation of the water molecule. The former overestimates the interaction while the latter underestimates it. Xantheas *et al.*[23] reported that BSSE of the water dimer is 0.83 kcal mol^{-1} (MP2/aug-cc-pVDZ) at the optimized configuration including the deformation of the molecules. This could be regarded as the maximum limit of the error since the value must be averaged over the various configuration.

ACKNOWLEDGMENTS

This work is financially supported in part by the Global Environment Research Fund (project B-2) of Ministry of the Environment of Japan, and Grant-in Aid for Scientific Research on Priority Areas "Water and biomolecules" (430-18031019) and "Molecular Theory for Real Systems" (461) of Ministry of Education, Culture, Sports, Science and Technology of Japan.

[1] K. Pfeilsticker, A. Lotter, C. Peters, and H. Bosch, Science **300**, 2078 (2003).
[2] B. Sierk, S. Solomon, J. S. Daniel, R. W. Portmann, S. I. Gutman, A. O. Langford, C. S. Eubank, E. G. Dutton, and K. H. Holub, J. Geophys. Res. **109**, D08307 (2004).
[3] L. A. Curtiss, D. J. Frurip, and M. Blander, J. Chem. Phys. **71**, 2703 (1979).
[4] H. A. Gebbie, W. J. Burroughs, J. Chamberlain, J. E. Harries, and R. G. Jones, Nature (London) **221**, 143 (1969).
[5] V. I. Dianov-Klokov, V. M. Ivanov, V. N. Arefev, and N. I. Sizov, J. Quant. Spectrosc. Radiat. Transf. **25**, 83 (1981).
[6] G. V. Bondarenko and Y. E. Gorbaty, Mol. Phys. **74**, 639 (1991).
[7] Y. S. Jin and S. Ikawa, J. Chem. Phys. **119**, 12432 (2003).
[8] J. G. Cormier, J. T. Hodges, and J. R. Drummond, J. Chem. Phys. **122**, 114309 (2005).
[9] P. Bandyopadhyay, S. Ten-no, and S. Iwata, Mol. Phys. **96**, 349 (1999).
[10] R. S. Fellers, C. Leforestier, L. B. Barly, M. G. Brown, and R. J. Saykally, Science **284**, 945 (1999).
[11] E. M. Mas, R. Bukowski, K. Szalewicz, G. C. Groenenboom, P. E. S.

Wormer, and A. van der Avoird, J. Chem. Phys. **113**, 6687 (2000).
[12] H. R. Barry, L. Corner, G. Hancock, R. Peverall, T. L. Ranson, and G. A. D. Ritchie, Phys. Chem. Chem. Phys. **5**, 3106 (2003).
[13] T. Nakayama, H. Fukuda, A. Sugita, S. Hashimoto, M. Kawasaki, S. Aloisio, I. Morino, and G. Inoue, Chem. Phys. **334**, 196 (2007).
[14] S. Nakamichi, Y. Kawaguchi, H. Fukuda, S. Enami, S. Hashimoto, M. Kawasaki, T. Umekawa, I. Morino, H. Suto, and G. Inoue, Phys. Chem. Chem. Phys. **8**, 364 (2006).
[15] J. Mrazek and J. V. Burda, J. Chem. Phys. **125**, 194518 (2006).
[16] L. S. Rothman *et al.*, J. Quant. Spectrosc. Radiat. Transf. **96**, 139 (2005).
[17] R. A. Toth, J. Quant. Spectrosc. Radiat. Transf. **94**, 1 (2005).
[18] X. Liu, X. Zhou, J. B. Jeffries, and R. K. Hanson, J. Quant. Spectrosc. Radiat. Transf. **103**, 565 (2007).
[19] H.-M. Lin, M. Seaver, K. Y. Tang, A. E. W. Knight, and C. S. Parmenter, J. Chem. Phys. **70**, 5442 (1979).
[20] C. S. Parmenter and M. Seaver, J. Chem. Phys. **70**, 5458 (1979).
[21] K. T. Tang and J. P. Toennies, J. Chem. Phys. **118**, 4976 (2003).
[22] The Monte Carlo simulations show evident temperature dependency. The averaged interaction energies evaluated with a lower level of *ab initio* molecular method [Hartree-Fock/6-31G(d,p)] are −5.2 kcal/mol (50 K), −4.8 kcal/mol (100 K), −4.5 kcal/mol (150 K), and −3.9 kcal/mol (200 K).
[23] S. S. Xantheas, C. J. Burnham, and R. J. Harrison, J. Chem. Phys. **116**, 1493 (2002).